Applied Catalysis B: Environmental 126 (2012) 258–264

Contents lists available at SciVerse ScienceDirect

Applied Catalysis B: Environmental

journal homepage: www.elsevier.com/locate/apcatb

Dissolution of mesoporous silica supports in aqueous solutions: Implications for mesoporous silica-based water treatment processes

Anh Le-Tuan Pham[a], David L. Sedlak[a,**], Fiona M. Doyle[b,*]

[a] Department of Civil and Environmental Engineering, University of California, Berkeley, Berkeley, CA 94720, United States
[b] Department of Materials Science and Engineering, University of California, Berkeley, Berkeley, CA 94720, United States

ARTICLE INFO

Article history:
Received 6 March 2012
Received in revised form 13 June 2012
Accepted 19 July 2012
Available online 27 July 2012

Keywords:
Mesoporous silica
Hydrogen peroxide
Fenton reaction
Advanced oxidation process
Silica solubility in water

ABSTRACT

Under pH 7–10 conditions, the mesoporous silica supports proposed for use in water treatment are relatively unstable. In batch experiments conducted in pH 7 solutions, the commonly used support SBA-15 dissolved quickly, releasing approximately 30 mg/L of dissolved silica after 2 h. In column experiments, more than 45% of an initial mass of 0.25 g SBA-15 dissolved within 2 days when a pH 8.5 solution flowed through the column. In a mixed iron oxide/SBA-15 system, the dissolution of SBA-15 changed the iron oxide reactivity toward H_2O_2 decomposition, because dissolved silica deposited on iron oxide surface and changed its catalytic active sites. As with SBA-15, other mesoporous silica materials including HMS, MCM-41, four types of functionalized SBA-15, and two types of metal oxide-containing SBA-15 also dissolved under circumneutral pH solutions. The dissolution of mesoporous silica materials raises questions about their use under neutral and alkaline pH in aqueous solutions, because silica dissolution might compromise the behavior of the material.

1. Introduction

Owing to their high surface area and unique nano-porous structure, ordered mesoporous silica supports (e.g., SBA-15 and MCM-41) have been proposed for water remediation [1]. For example, functionalized mesoporous silica has been used as an adsorbent for toxic metals [2,3], anions [4,5], radionuclides [6] and various organic contaminants [7–10]. Mesoporous silica catalysts impregnated with metal oxides, such as iron-, manganese- and copper-containing SBA-15, have also been used in hydrogen peroxide-based oxidative water treatment [11–13]. Many of these applications employ aqueous solutions at circumneutral pH values despite the fact that silica is relatively soluble under these conditions. Given the high surface area and poor crystalinity of these materials it is possible that they will dissolve rapidly in water. If so, the use of these materials in aqueous media needs to be carefully evaluated because the dissolution of functionalized mesoporous silica adsorbents could release adsorbed species and the organic functional compounds, many of which are toxic to aquatic life. Silica dissolution could also affect the long-term performance of the catalyst. Moreover, the presence of the dissolved silica species might lead to unexpected changes in the catalyst surface as silica interacts with catalytic active sites [14].

Previous investigators have reported dissolved silica concentration in excess of 100 mg/L when mesoporous silica materials were suspended in solutions at pH values between 5 and 6 [15,16]. Measurement of the dissolution of $SiO_{2(s)}$ indicates that the mineral's solubility and dissolution rate are sensitive to pH, with higher solubility and faster dissolution observed in neutral and alkaline solutions [17]. To understand the stability of mesoporous silica supports, it is important to know the effect of pH on its dissolution rate. However, to the best of our knowledge, such information has not been reported. Here we have investigated the dissolution rate of three widely used types of mesoporous silica, namely SBA-15, HMS and MCM-41, in aqueous solutions at environmentally relevant pH values (pH 7–10). Recognizing the possibility that functionalized organic groups or precipitated oxides might significantly modify the aqueous solubility of silica [18], the dissolution of SBA-15 functionalized with different organic compounds (i.e., propylthiol-, aminopropyl-, ethyldiaminopropyl- and diethylentriaminopropyl-) or SBA-15 that was coated with iron and aluminum oxide were also investigated. Because we observed the rapid release of dissolved silica in all cases, we also investigated how the presence of dissolved silica might change the catalytic activity of the iron oxide/SBA-15 system toward H_2O_2 decomposition.

* Corresponding author. Tel.: +1 510 333 1693; fax: +1 510 643 5792.
** Corresponding author. Tel.: +1 510 643 0256; fax: +1 510 642 7483.
E-mail addresses: sedlak@berkeley.edu (D.L. Sedlak), fmdoyle@berkeley.edu (F.M. Doyle).

0926-3373/$ – see front matter © 2012 Elsevier B.V. All rights reserved.
http://dx.doi.org/10.1016/j.apcatb.2012.07.018

2. Experimental

2.1. Synthesis of mesoporous silica supports

SBA-15, HMS and MCM-41 were synthesized following procedures reported elsewhere [19–21]. Iron oxide- and aluminum oxide-containing SBA15 (SBA15-Fe-oxide and SBA15-Al-oxide) was synthesized following the procedure described by Gervasini et al. [22]. Briefly, 1 g of SBA-15 was suspended in a 120 mL solution of 1:1 water:propanol-1. The solution pH was kept at 10 with ammonium hydroxide and the temperature was maintained at 0 °C using an ice bath. Iron and aluminum precusor solutions, prepared by dissolving 0.015 mol of either iron-acetylacetonate or aluminum-acetylacetonate in a 500 mL solution of 1:1 water:propanol-1, were gently dropped into the SBA-15 solution. The mixtures were then removed from the ice bath and vigorously stirred at room temperature. The solids were recovered by filtration, air dried at 100 °C for 24 h and calcined at 500 °C for 4 h. All solutions were prepared using 18 MΩ Milli-Q water from a Millipore system.

SBA-15 functionalized with propylthiol-, aminopropyl-, ethyldiaminopropyl- and diethylenetriaminopropyl- were synthesized following the procedure reported by Aguado et al. [23,24]. Briefly, 4 g of triblock copolymer P123 was dissolved in a solution of 125 mL of 1.9 M HCl and the mixture was heated to 40 °C. Subsequently, 8.2 g tetraethyl orthosilicate was added and the mixture was vigorously stirred for 45 min, followed by the addition of 2 mmol of (3-mercaptopropyl)trimethoxysilane (for propylthiol-SBA15), 4.1 mmol 3-aminopropyltrimethoxysilane (for aminopropyl-SBA15), N-[3-(trimethoxysilyl)propyl]-ethylenediamine (for ethyldiaminopropyl-SBA15) or 3-[2-(2-aminoethylamino)ethylamino]propyl-trimethoxysilane (for diethylentriaminopropyl-SBA15). The mixture was stirred for 20 h at 40 °C, then aged under static condition at 100 °C for 24 h. The functionalized-SBA15 was filtered and the P123 template was extracted by refluxing in ethanol for 24 h.

2.2. Characterization

The surface area of mesoporous silica supports was determined using the 5 point BET (Brunauer–Emmett–Teller) nitrogen physisadsorption method. The measurements were made in the linear part of the isotherm where the BET equation is valid, namely in the pressure range of $0.06 < p/p_0 < 0.2$. The iron and aluminum content of SBA15-Fe-oxide and SBA15-Al-oxide were measured by dissolving the solids in concentrated HCl and measuring dissolved Fe and Al in the solution phase using an Inductively Coupled Plasma-Optical Emission Spectrometer (ICP-OES). The SBA15-Fe-oxide and SBA15-Al-oxide contained 9 wt.% of Fe and 4.7 wt.% of Al, respectively. The morphology of the solids was determined using a Philips CM200/FEG transmission electron microscope (TEM) at 200 kV and Zeiss Evo 10 scanning electron microscope (SEM) at 5 kV. X-ray diffraction (XRD) analysis was performed with Cu Kα radiation using a Panalytical 2000 diffractometer.

2.3. Dissolution

Batch experiments. All experiments were carried out at 25 ± 1 °C in a 50 mL polypropylene flask open to the atmosphere. 50 mg of solid was added to 50 mL Milli-Q water and the suspension was vigorously stirred. The initial solution pH was adjusted using 1 M NaOH or 0.5 M H_2SO_4. Although sulfate can accelerate silica dissolution [25], this effect is only important in the presence of significant amount of sulfate (e.g., 0.1 M SO_4^{2-} in Ref. [25]). The maximum sulfate concentration in all of our experiments was approximately 50 μM and, therefore, its effect on silica dissolution is likely minimal. Solutions with pH 7 were buffered with 1 mM of either piperazine-N,N′-bis(ethanesulfonic acid) (PIPES), bicarbonate or phosphate. Preliminary results indicated that the dissolution of SBA-15 was not affected by buffer types (see Fig. S1 in Supporting Information). Therefore, PIPES was used in all subsequent experiments. The use of PIPES, an organic buffer that does not adsorb on iron oxide surface or forms complexes with dissolved iron [26], allowed us to investigate the role of dissolved silica toward iron oxide reactivity (Section 3.5). Solutions with pH 8–9 were buffered by 4 mM borate, while solutions with an initial pH of 10 were unbuffered. Samples were withdrawn at pre-determined time intervals, filtered immediately through a 0.2 μm nylon filter and analyzed for dissolved SiO_2.

Column experiments with SBA-15. Experiments were conducted in 10 mm ID glass columns. No dissolution of the column glass wall was detected in the control experiment. 0.25 g SBA-15 was packed in the column and a pH 8.5 solution (buffered by 12 mM borate) was passed through the columns at a flow rate of 0.5 mL/min in a downward direction. The hydraulic retention time was ca. 0.4 min. A 0.45 μm nylon filter was attached to the outlet of the column to prevent elution of the solid out of the column (0.45 μm filter was used instead of 0.2 μm filter to avoid high back-pressure in the column). The concentration of dissolved SiO_2 in the column effluent was continuously measured throughout the course of the experiment.

2.4. Reactivity of iron oxide/SBA15 toward H_2O_2 decomposition

The effect of dissolution of SBA-15 on amorphous iron oxyhydroxide (Fe-$ox_{(s)}$, Aldrich) reactivity toward catalytic decomposition of H_2O_2 was investigated in both batch and column experiments. In batch experiments, the reactions were initiated by adding an aliquot of H_2O_2 stock solution to a pH-adjusted solution containing 1 g/L SBA-15 and 1 g/L Fe-$ox_{(s)}$. Samples were withdrawn at pre-determined time intervals and filtered immediately through a 0.2 μm nylon filter and analyzed for dissolved SiO_2 and H_2O_2. In column experiments, Fe-$ox_{(s)}$ and SBA-15 were packed in the column in different configurations (Fig. 1), and pH 8.5 solution containing 5 mM H_2O_2 was passed through at a flow rate of 0.5 mL/min. The concentration of dissolved SiO_2 and H_2O_2 in the solution at the outlet was measured at a predetermined time interval.

2.5. Analytical methods

H_2O_2 was analyzed spectrophotometrically by the titanium sulfate method [27]. In the absence of H_2O_2, dissolved silica was measured either spectrophotometrically by the molybdosilicate method [28] or by ICP-OES. The molybdosilicate method only detects dissolved silica monomer and not other forms of silica (e.g., SiO_2 in polymer forms or nano-sized SiO_2 particles), while the method using ICP-OES detects all forms of silica, including the particulate silica that passed through the filter. Two methods gave similar results (i.e., $[SiO_2]_{molydosilicate} \sim 95\% [SiO_2]_{ICP\text{-}OES}$), indicating that minimal particulate silica was able to pass through the filter. ICP-OES was used to measure dissolved silica in the presence of H_2O_2, as interference from H_2O_2 precludes silica measurement by the molybdosilicate method. The deposition of SiO_2 on the Fe-$ox_{(s)}$ surface in column experiment was confirmed by using SEM with an EDAX Genesis energy dispersive X-ray unit (SEM-EDX).

To investigate the contribution of dissolved iron (leached from Fe-$ox_{(s)}$) toward H_2O_2 decomposition, total dissolved iron was quantified using the 1,10-phenanthroline method [29] after adding hydroxylamine hydrochloride to the filtered samples. The concentration of dissolved iron was always below the detection limit (i.e., less than 5 μM), indicating that the amount of H_2O_2 decomposed

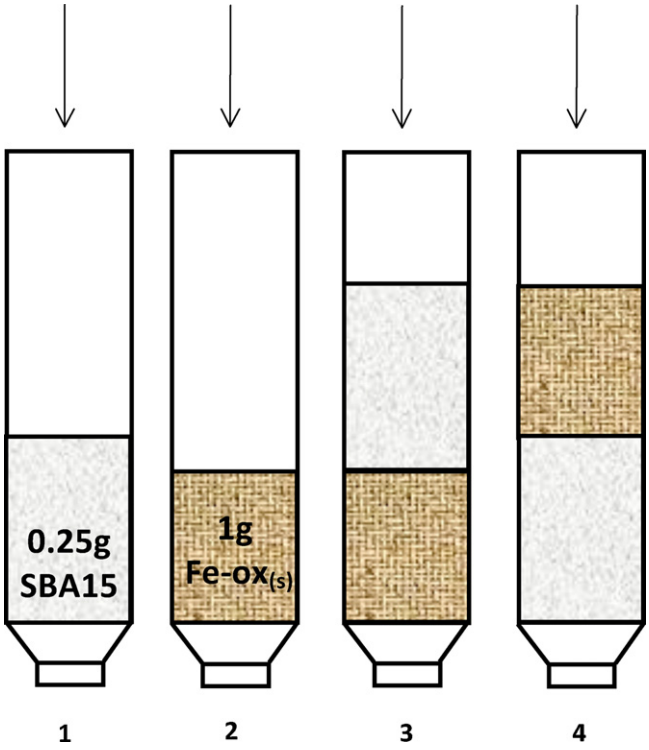

Fig. 1. Investigation of H_2O_2 decomposition in column experiments (column ID = 10 mm). Columns 1 and 2 contained only 0.25 g SBA-15 or 1 g Fe-ox$_{(s)}$, respectively. Column 3 contained SBA-15 that was on the top of Fe-ox$_{(s)}$ while in column 4 Fe-ox$_{(s)}$ was on the top of SBA-15.

by dissolved iron was negligible compared with that catalyzed by iron oxide surface.

All experiments were carried out at least in triplicate and average values along with one standard deviation are presented.

3. Results and discussion

3.1. Materials characterization

The BET surface area of the 9 mesoporous silica supports ranged from approximately 330 to 800 m^2/g (Table 1), and the measured C values of the BET equation were between 50 and 250. The TEM micrographs, reported in the Supporting Information (Fig. S2), indicated that functionalization did not modify the mesoporous structure of the supports.

3.2. Dissolution of SBA-15 in batch experiments

The dissolution of SBA-15 was investigated in well-mixed batch solutions containing 1 g/L SBA-15 (Fig. 2). At pH values above 7, between 20 and 55 mg/L of dissolved silica (based on SiO_2) was

Table 1
BET surface area of mesoporous silica supports.

Materials	BET surface area (m^2/g)
SBA-15	636
HMS	804
MCM-41	501
SBA15-PT	334
SBA15-AP	570
SBA15-ED	530
SBA15-DT	380
SBA15-Fe-oxide	524
SBA15-Al-oxide	373

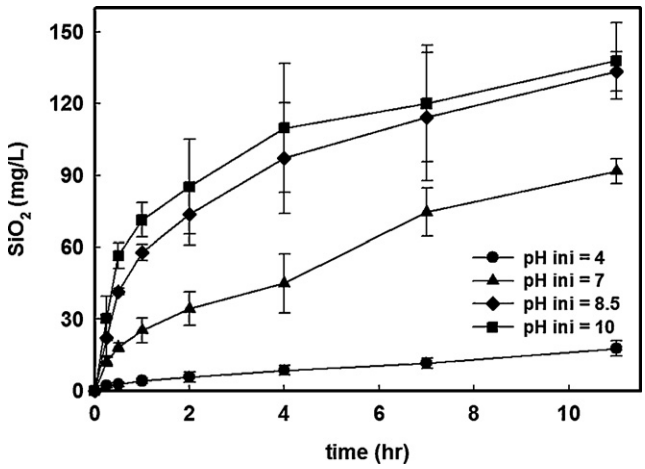

Fig. 2. Dissolution of SBA-15 in well-mixed batch solution, 1 g/L SBA-15, $pH_{final} = 4.1 \pm 0.1, 7 \pm 0.1, 8.1 \pm 0.1$ and 8.6 ± 0.4 for $pH_{initial}$ of 4, 7, 8.5 and 10, respectively. Solutions with $pH_{initial}$ of 7 and 8.5 were buffered with 1 mM PIPES and 4 mM borate, respectively.

released during the first 30 min. The dissolved silica concentration continued to increase throughout the 11 h experiments, with no indication of saturation. The release of silica was attributable to the following reactions:

$$SiO_2 + 2H_2O \rightarrow H_4SiO_4\,(pK_{s0} = 2.74)\,[17] \quad (1)$$

$$H_4SiO_4 \Leftrightarrow H_3SiO_4^- + H^+\,(pK_{a1} = 9.84)\,[17] \quad (2)$$

The predicted concentration of dissolved silica in equilibrium with amorphous $SiO_{2(s)}$ at pH values between 7 and 9 is between 120 and 140 mg/L [17]. The dissolution of amorphous $SiO_{2(s)}$ in general, however, is a relatively slow process. Therefore, the rapid dissolution of SBA-15 is attributable to its high surface area and the unique wall and pore structure that provide convex surfaces with small radii of curvature, at which the activity of the amorphous silica exceeds that of the bulk material. The TEM and SEM micrographs (Figs. 3 and S3, respectively), and XRD pattern (Fig. S4) of the material that underwent the dissolution test were similar to those of the original SBA-15.

3.3. Dissolution of HMS, MCM-41 and modified mesoporous supports.

The dissolution of HMS and MCM-41, as well as modified materials such as propylthiol-, aminopropyl-, ethyldiaminopropyl-, diethylentriaminopropyl-functionalized SBA-15 (SBA15-PT, SBA15-AP, SBA15-ED and SBA15-DT, respectively), iron oxide-containing SBA-15 (SBA15-Fe-oxide) and alumina-containing SBA-15 (SBA15-Al-oxide) in pH 7 batch solution was also investigated. In these systems, the amount of dissolved silica released after a period of 4 h ranged from approximately 7 mg/L (in the case of SBA15-Al-oxide) to 133 mg/L (in the case of SBA15-AP) (Fig. 4, top). The concentration of dissolved silica in the SBA15-AP system exceeded the solubility of silica at pH 7 (i.e., 120 mg/L [17]), suggesting that the solution was supersaturated with respect to amorphous $SiO_{2(s)}$. This phenomenon was also observed in a previous study with MCM-41 [15].

To gain insights into the relative stability among the mesoporous silica materials, their initial rate of dissolution in the batch experiment was calculated by normalizing the amount of dissolved silica released during the first 30 min against the materials' surface area. Despite the differences in the synthesis method (Table S1, Supporting Information), SBA-15, HMS and MCM-41 dissolved at comparable rates (i.e., ca. 3×10^{-3} to 4×10^{-3} mg m^{-2} h^{-1},

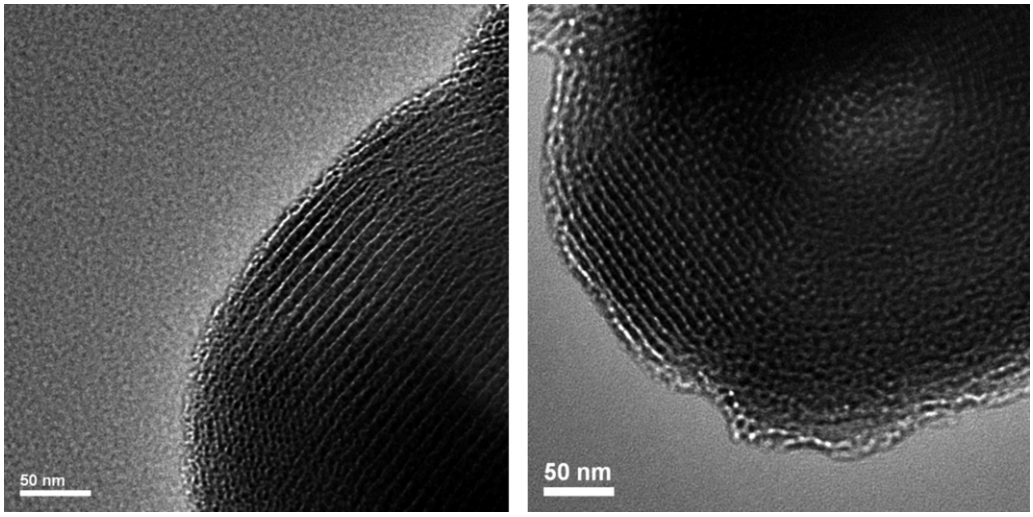

Fig. 3. TEM images of SBA-15 recovered from the pH 8.5 solution after 20 h. The original pore structure of the material was well observed.

Fig. 4, bottom). Regarding the modified materials, three types of aminoalkyl-functionalized SBA-15 (namely SBA15-AP, SBA15-ED and SBA15-DT) dissolved at an initial rate that was approximately 1.5–3 times faster than that of SBA-15, HMS and MCM-41. In contrast, SBA15-PT, SBA15-Fe-oxide, and SBA15-Al-oxide dissolved 3–20 times slower than SBA-15, HMS and MCM-41 (Fig. 4, bottom). The most stable material in this study was SBA15-Al-oxide (the initial dissolution rate of 2×10^{-4} mg m^{-2} h^{-1}). The effect of alumina on the stability of amorphous silica has been widely reported in the literature [18,30,31], although the mechanism through which alumina stabilizes silica remains unclear. The role of the iron oxide and propylthiol functional group on the enhanced stability of the SBA-15 support was also unclear. Regarding the aminoalkyl-functionalized SBA-15, faster dissolution of these materials was probably due to a high localized pH at the silica surface due to the basic nature of the amine groups (the pK_a of aliphatic amines is above 10). Consequently, higher local pH values might cause faster dissolution and higher solubility of these materials.

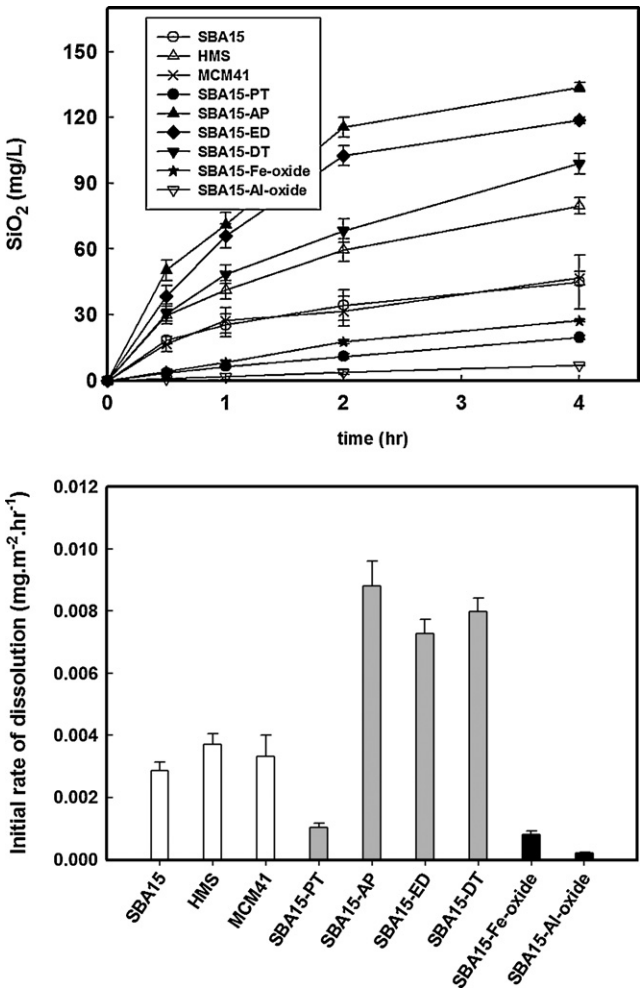

Fig. 4. Dissolution of various mesoporous silica-based supports in well-mixed batch solution (top), and initial rates of dissolution during the first 30 min of the experiments (bottom). [solid] = 1 g/L, pH = 7 ± 0.1, buffered with 1 mM PIPES.

3.4. Long-term stability of SBA-15 in column experiment

The long term stability of SBA-15 was further investigated in a column experiment in which a pH 8.5 solution was passed continuously at 0.5 mL/min through SBA-15 packed in a 10 mm diameter column. The concentration of dissolved silica at the column outlet decreased gradually during the first 8.5 h from more than 200 mg/L

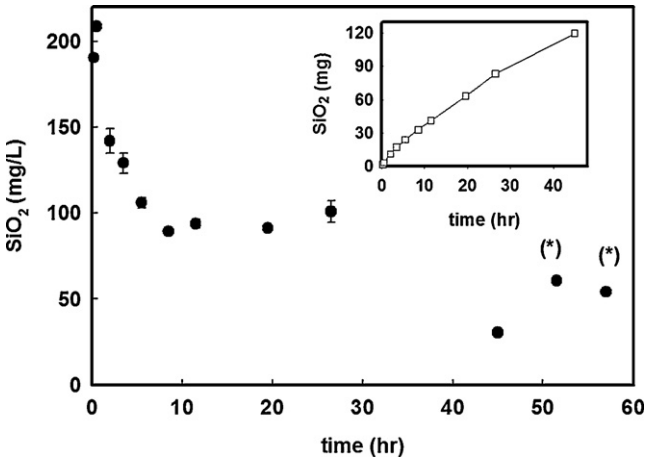

Fig. 5. Column experiment containing 250 mg SBA-15. Flow rate = 0.5 mL/min, pH = 8.5, buffered with 12 mM borate. Inset: calculated cumulative amount of dissolved silica. (*) These data point were taken after the SBA-15 bed was compressed at t = 45 h (see Fig. 6 for detailed explanation).

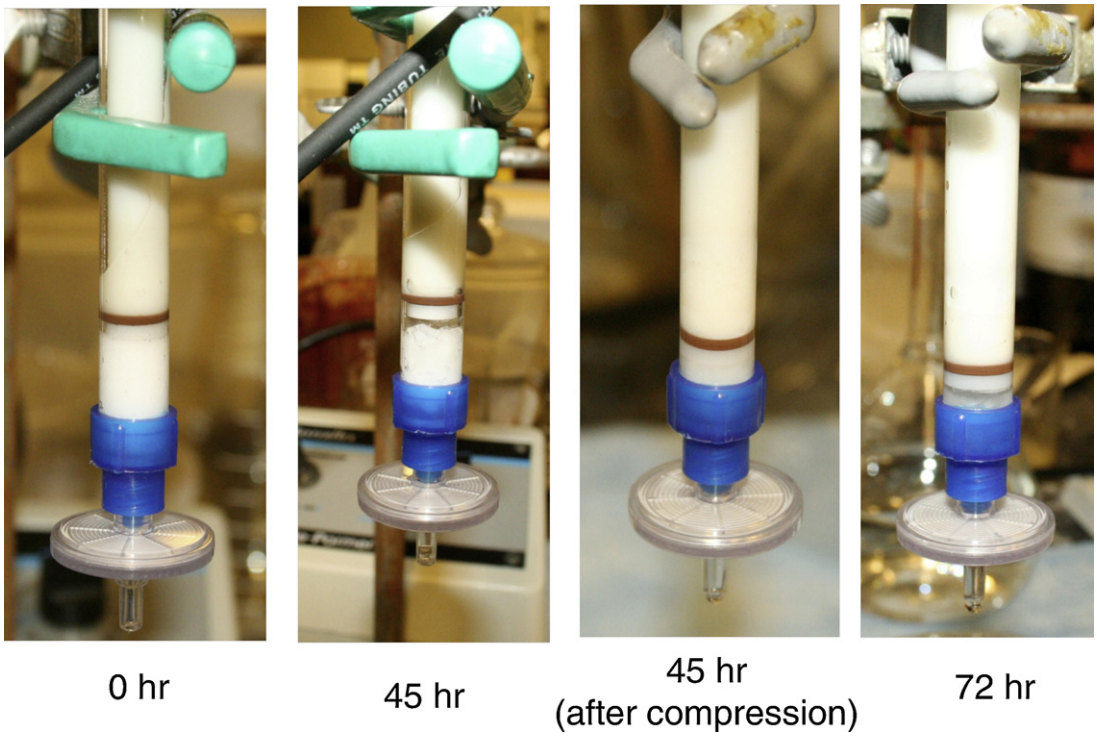

Fig. 6. Dissolution of SBA-15 in the column experiment. After 45 h, a significant amount of SBA-15 was dissolved. The remaining SBA-15 bed was then compressed in order to eliminate the void space in the column. Further dissolution created the void space again (figure for t = 72 h).

to approximately 90 mg/L then remained at this value for the next 18 h (Fig. 5). The higher-than-predicted concentration (i.e., 120–140 mg/L [17]) observed initially was attributable to supersaturation with respect to amorphous $SiO_{2(s)}$. Approximately 120 mg of dissolved SiO_2 was recovered in the column effluent, which accounted for more than 45% of the initial mass of SBA-15 in the column (inset of Fig. 5). The disappearance of SBA-15 in the column due to dissolution was visually observed after 45 h (Fig. 6).

3.5. Impact of SBA-15 dissolution on reactivity of Fe-ox$_{(s)}$ in catalyzing H_2O_2 decomposition

Metal oxide-containing mesoporous silica catalysts have been used for H_2O_2-based oxidative water treatment [11–13]. However, the release of silica may alter the long term stability and reactivity of mesoporous silica-based catalysts, creating unexpected changes in the catalyst surface and hence the catalytic performance. To test this hypothesis, we studied the effect of SBA-15 dissolution on the kinetics of H_2O_2 decomposition catalyzed by Fe-ox$_{(s)}$ (reactions (3) and (4)) [32–34].

$$\equiv Fe^{2+} + H_2O_2 \rightarrow \equiv Fe^{3+} + {}^{\bullet}OH + OH^- \quad (3)$$

$$\equiv Fe^{3+} + H_2O_2 \rightarrow \equiv Fe^{2+} + HO_2^{\bullet} + H^+ \quad (4)$$

$$HO_2^{\bullet} \Leftrightarrow H^+ + O_2^{\bullet -} \quad (5)$$

This process was selected as a case study because of the popularity of metal oxide-impregnated mesoporous silica/H_2O_2 systems in

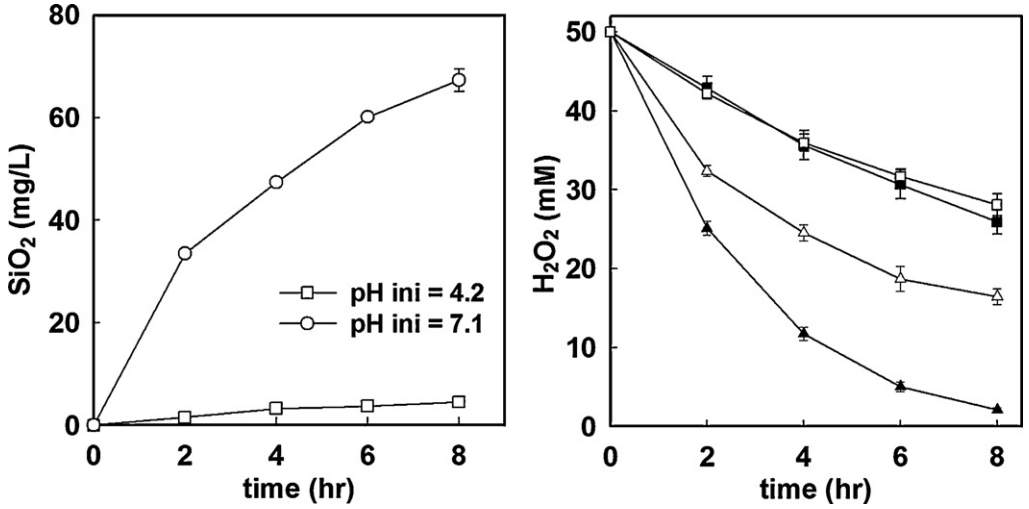

Fig. 7. Dissolved silica and H_2O_2 concentration in batch experiment. [Fe-ox$_{(s)}$] = 1 g/L, [SBA-15] = 1 g/L, $[H_2O_2]_{initial}$ = 50 mM. Solution with pH = 7 ± 0.1 was buffered with 1 mM PIPES. Squares: pH 4.2, triangles: pH 7 ± 0.1. Fe-ox$_{(s)}$ (filled symbol), Fe-ox$_{(s)}$ and SBA-15 (open symbol).

water treatment [13] and organic synthesis [35]. Organic solvents are often used in the latter application, but recent efforts to replace organic solvents with water have prompted interest in catalysts that are effective in water [36].

We studied the decomposition of H_2O_2 catalyzed by iron oxide in the presence of SBA-15. Although the catalytic activity of the iron oxide in this mixture does not represent that of iron-containing SBA-15 (where iron oxide is chemically deposited on the SBA-15 surface or is a part of the SBA-15 support), this approach allowed us to understand the role of dissolved silica released by SBA-15 unambiguously, which would not have been possible using iron-containing SBA-15.

In batch experiments, the rate of Fe-ox$_{(s)}$-catalyzed H_2O_2 decomposition was unaffected by the presence of SBA-15 at pH 4.2 ± 0.2, but significantly suppressed at pH 7.1 ± 0.1 (Fig. 7). Because SBA-15 is not redox active and does not cause H_2O_2 decomposition, this difference was attributed to the dissolution of silica at higher pH, followed by adsorption onto the surface of Fe-ox$_{(s)}$, occupying iron sites responsible for H_2O_2 decomposition, thereby diminishing the reactivity of Fe-ox$_{(s)}$ [14]. SBA-15 dissolution was much slower at the lower pH value, and not enough silica was adsorbed on Fe-ox$_{(s)}$ to alter the rate of H_2O_2 decomposition.

To confirm that the H_2O_2 decomposition was suppressed by deposition of dissolved silica onto the iron oxide rather than by some unanticipated interaction between SBA-15 and iron oxide, the catalytic decomposition of H_2O_2 was studied further using column experiments (Fig. 8). The H_2O_2 concentration at the outlet of column 1, containing only SBA-15, was unaffected by passage through the column because SBA-15 does not catalyze H_2O_2 decomposition. More than 97% of the initial H_2O_2 was decomposed as the solution passed through column 2 (containing only Fe-ox$_{(s)}$) and column 4 (in which the solution passed through the Fe-ox$_{(s)}$ before encountering SBA-15) due to reactions (3) and (4). For column 3 (in which the solution passed through SBA-15 before Fe-ox$_{(s)}$), the concentration of H_2O_2 increased gradually during the experiment as would be expected if the activity of the catalyst was decreasing over time.

Comparison of the dissolved silica concentrations leaving columns 1 and 3 indicates that the dissolved silica was adsorbed by Fe-ox$_{(s)}$, resulting in lower dissolved silica concentrations at the outlet of column 3. This adsorption was confirmed by SEM/EDS analysis of the Fe-ox$_{(s)}$ from column 3 after the test, which showed a Si peak (Fig. 9). With time, adsorption of dissolved silica lowered the catalytic activity of the Fe-ox$_{(s)}$ and therefore the H_2O_2 concentration at the outlet gradually increased.

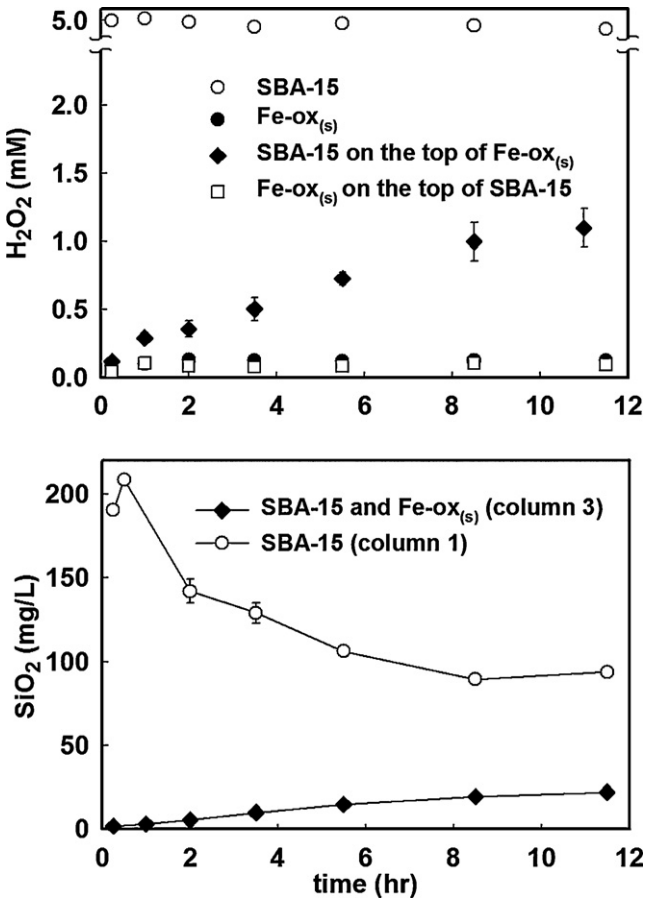

Fig. 8. Hydrogen peroxide and dissolved silica concentration at outlet of 10 mm ID columns through which pH = 8.5 ± 0.1 solutions containing 5 mM H_2O_2 were flowed at a 0.5 mL/min. Column was packed with 0.25 g SBA-15 and/or 1 g Fe-ox$_{(s)}$.

3.6. Dissolution of mesoporous silica supports – a broader implication.

In addition to being used in advanced oxidation processes for water treatment, mesoporous silica-based supports also have

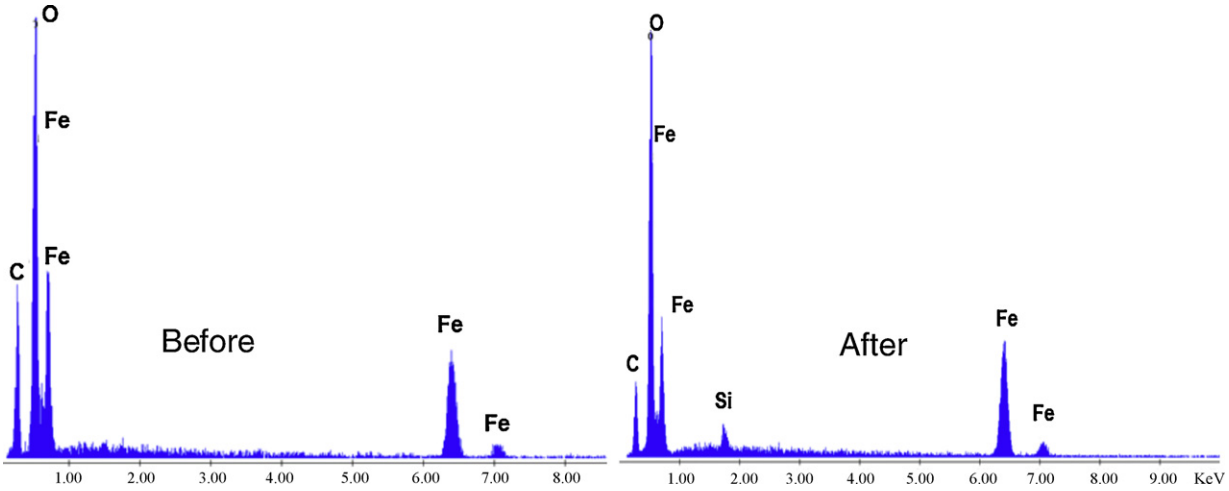

Fig. 9. EDS spectrum of the Fe-ox$_{(s)}$ surface before and after the column experiment. The Fe-ox$_{(s)}$ sample was collected from column 3 at the end of the experiment. The carbon peak is due to the carbon coating needed to prevent charging in the SEM.

been proposed for applications such as adsorption, separation, and sensing [7,37]. The results of our study, however, raise significant questions about the merits of their application in aqueous media. For example, when mesoporous silica is used to encapsulate enzymes and proteins [38], a process that is routinely conducted at pH values ranging from 5 to 11, significant dissolution of the substrate would be expected over a time scale of hours to days. Functionalized mesoporous silica also has been proposed as an adsorbent for removing toxic metals, anions, radionuclides and organic contaminants from polluted water. The dissolution of these adsorbents could release not only adsorbed contaminants but also the organic functional compounds, many of which are toxic to aquatic life. In addition, it was observed that adsorption of Cr(VI) [5] and organic contaminants [9] on various functionalized SBA-15 and HMS substrates was a pH dependent process, with lower adsorption affinity at neutral and alkaline pH. The dissolution of adsorbent might explain why adsorption capacity decreased at higher pH. Additional research is needed to evaluate the performance of mesoporous silica materials in these applications.

4. Conclusion

In summary, we have demonstrated that mesoporous silica materials such as SBA-15, HMS and MCM-41, four types of functionalized SBA-15, and iron and aluminum oxide-containing SBA-15 are unstable in aqueous solution, especially at circumneutral and more basic pH values. The results raise questions about the use of these materials in aqueous-based applications such as adsorption and catalysis, suggesting that these materials may only be suitable under acidic conditions, where silica dissolves slowly. We also showed that silica dissolved from mesoporous silica supports such as SBA-15 may change the reactivity of catalysts. Our experiments have shown that silica-containing iron oxide, produced from adsorption of dissolved silica on Fe-ox$_{(s)}$, was less active in catalyzing the decomposition of H_2O_2 than pure iron oxide.

Among the studied materials, the SBA-15 support that was functionalized with propylthiol or contained iron or aluminum oxide was more stable than the bare SBA-15. Although the mechanism through which the propylthiol group and metal oxides enhance the stability of silica is still unclear, our findings suggest that it might be possible to design more stable mesoporous silica based materials. Given the complex nature of functional group/metal center and support interaction, additional research is required to further investigate this issue.

Supporting information available

Mesoporous silica substrates synthesis methods, TEM and SEM images, XRD data.

Acknowledgements

This research was supported by the U.S. National Institute for Environmental Health Sciences (NIEHS) Superfund Basic Research Program (Grant P42 ES004705). A.L.P. was supported in part by Vietnam Education Foundation (VEF). The authors acknowledge support of the National Center for Electron Microscopy, Lawrence Berkeley National Laboratory, which is supported by the U.S. Department of Energy under Contract # DE-AC02-05CH11231. We thank Benjamin Legg (Jillian Banfield research group, UC Berkeley) for assisting with BET analysis.

Appendix A. Supplementary data

Supplementary data associated with this article can be found, in the online version, at http://dx.doi.org/10.1016/j.apcatb.2012.07.018.

References

[1] C. Cooper, R. Burch, Water Research 33 (1999) 3689–3694.
[2] A.M. Burke, J.P. Hanrahan, D.A. Healy, J.R. Sodeau, J.D. Holmes, M.A. Morris, Journal of Hazardous Materials 164 (2009) 229–234.
[3] H. Yang, R. Xu, X. Xue, F. Li, G. Li, Journal of Hazardous Materials 152 (2008) 690–698.
[4] E. McKimmy, J. Dulebohn, J. Shah, T.J. Pinnavaia, Chemical Communications (2005) 3697–3699.
[5] J. Li, L. Wang, T. Qi, Y. Zhou, C. Liu, J. Chu, Y. Zhang, Microporous and Mesoporous Materials 110 (2008) 442–450.
[6] W. Yantasee, G.E. Fryxell, R.S. Addleman, R.J. Wiacek, V. Koonsiripaiboon, K. Pattamakomsan, V. Sukwarotwat, J. Xu, K.N. Raymond, Journal of Hazardous Materials 168 (2009) 1233–1238.
[7] A. Walcarius, L. Mercier, Journal of Materials Chemistry 20 (2010) 4478–4511.
[8] M. Anbia, M. Lashgari, Chemical Engineering Journal 150 (2009) 555–560.
[9] D. Zhu, H. Zhang, Q. Tao, Z. Xu, S. Zheng, Environmental Toxicology and Chemistry 28 (2009) 1400–1408.
[10] R. Sawicki, L. Mercier, Environmental Science and Technology 40 (2006) 1978–1983.
[11] G. Calleja, J.A. Melero, F. Martiïnez, R. Molina, Water Research 39 (2005) 1741.
[12] Y.-F. Han, F. Chen, K. Ramesh, Z. Zhong, E. Widjaja, L. Chen, Applied Catalysis B: Environmental 76 (2007) 227–234.
[13] S. Navalon, M. Alvaro, H. Garcia, Applied Catalysis B: Environmental 99 (2010) 1–26.
[14] A.L.-T. Pham, F.M. Doyle, D.L. Sedlak, Environmental Science and Technology 46 (2012) 1055–1062.
[15] C.P. Guthrie, E.J. Reardon, The Journal of Physical Chemistry A 112 (2008) 3386–3390.
[16] A. Galarneau, M. Nader, F. Guenneau, F. Di Renzo, A. Gedeon, The Journal of Physical Chemistry C 111 (2007) 8268–8277.
[17] R.K. Iler, The Chemistry of Silica: Solubility, Polymerization, Colloid and Surface Properties, and Biochemistry, 1979.
[18] D.R. Dunphy, S. Singer, A.W. Cook, B. Smarsly, D.A. Doshi, C.J. Brinker, Langmuir 19 (2003) 10403–10408.
[19] D. Zhao, J. Feng, Q. Huo, N. Melosh, G.H. Fredrickson, B.F. Chmelka, G.D. Stucky, Science 279 (1998) 548–552.
[20] P.T. Tanev, T.J. Pinnavaia, Science 267 (1995) 865–867.
[21] J.S. Beck, J.C. Vartuli, W.J. Roth, M.E. Leonowicz, C.T. Kresge, K.D. Schmitt, C.T.W. Chu, D.H. Olson, E.W. Sheppard, Journal of the American Chemical Society 114 (1992) 10834–10843.
[22] A. Gervasini, C. Messi, P. Carniti, A. Ponti, N. Ravasio, F. Zaccheria, Journal of Catalysis 262 (2009) 224–234.
[23] J. Aguado, J.M. Arsuaga, A. Arencibia, Industrial and Engineering Chemistry Research 44 (2005) 3665–3671.
[24] J. Aguado, J.M. Arsuaga, A. Arencibia, M. Lindo, V. Gascón, Journal of Hazardous Materials 163 (2009) 213–221.
[25] S. Bai, S. Urabe, Y. Okaue, T. Yokoyama, Journal of Colloid and Interface Science 331 (2009) 551–554.
[26] Q. Yu, A. Kandegedara, Y. Xu, D.B. Rorabacher, Analytical Biochemistry 253 (1997) 50–56.
[27] G. Eisenberg, Industrial and Engineering Chemistry Analytical Edition 15 (1943) 327.
[28] A.E. Green Berg, L.S. Clesceri, A.D. Eaton, Standard methods for the examination of water and wastewater (1992).
[29] H. Tamura, K. Goto, T. Yotsuyanagi, M. Nagayama, Talanta 21 (1974) 314.
[30] B.R. Bickmore, K.L. Nagy, A.K. Gray, A.R. Brinkerhoff, Geochimica et Cosmochimica Acta 70 (2006) 290–305.
[31] B.W. Glasspoole, J.D. Webb, C.M. Crudden, Journal of Catalysis 265 (2009) 148–154.
[32] S.-S. Lin, M.D. Gurol, Environmental Science and Technology 32 (1998) 1417–1423.
[33] J.J. Pignatello, E. Oliveros, A. MacKay, Critical Reviews in Environmental Science and Technology 36 (2006) 1.
[34] A.L.-T. Pham, C. Lee, F.M. Doyle, D.L. Sedlak, Environmental Science and Technology 43 (2009) 8930–8935.
[35] L. Wang, A. Kong, B. Chen, H. Ding, Y. Shan, M. He, Journal of Molecular Catalysis A: Chemical 230 (2005) 143–150.
[36] S. Minakata, M. Komatsu, Chemical Reviews 109 (2009) 711–724.
[37] B. Melde, B. Johnson, P. Charles, Sensors 8 (2008) 5202–5228.
[38] M. Hartmann, Chemistry of Materials 17 (2005) 4577–4593.